CHEMISTRY
A EUROPEAN JOURNAL

FULL PAPER

DOI: 10.1002/chem.200600289

One-dimensional arrangement of Mn^{III} salen and a TCNQ radical with single-chain magnet behavior

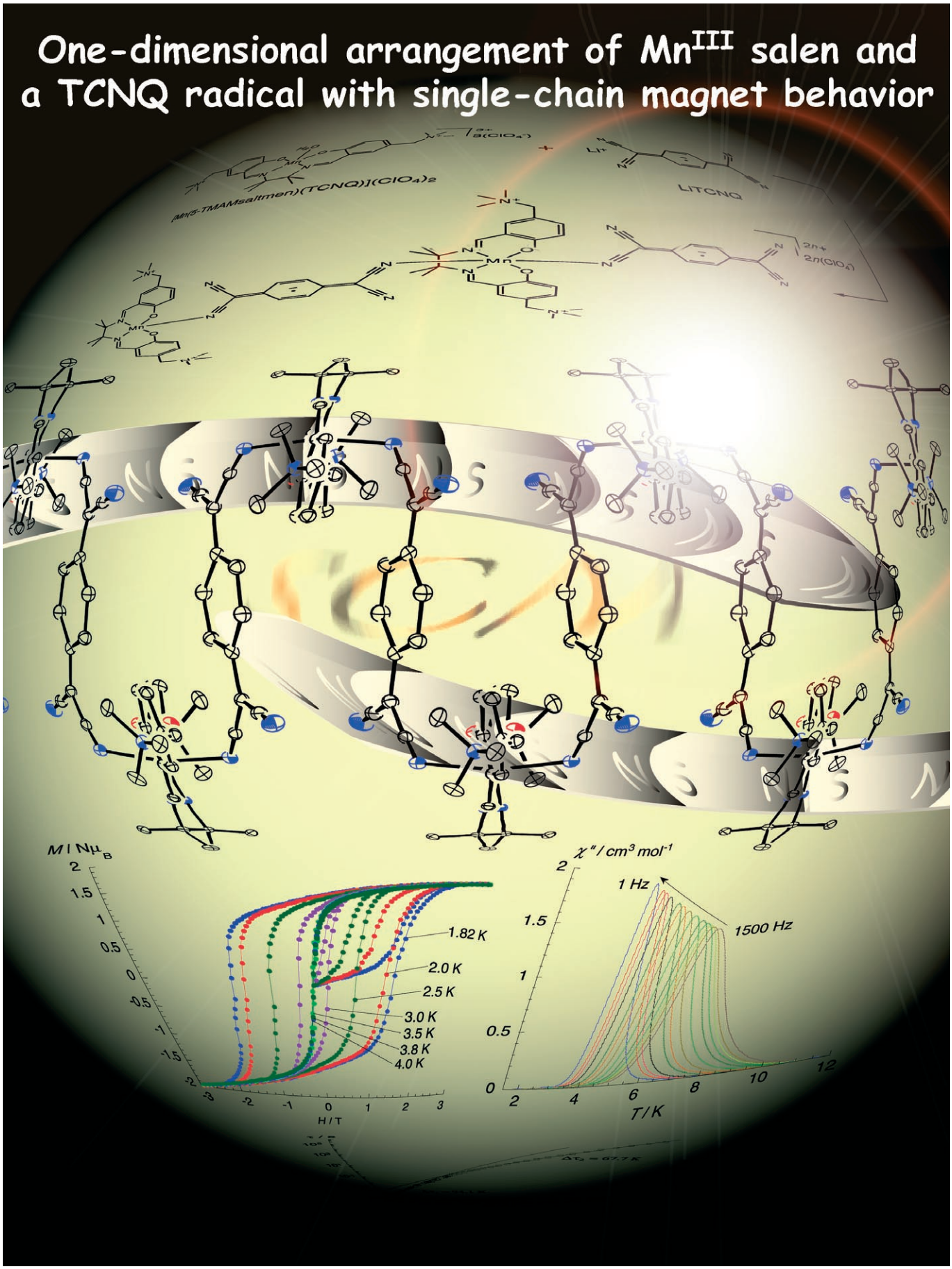

VIP

Single-Chain Magnet Behavior in an Alternated One-Dimensional Assembly of a Mn^{III} Schiff-Base Complex and a TCNQ Radical**

Hitoshi Miyasaka,*[a, g] Tomokura Madanbashi,[a] Kunihisa Sugimoto,[b] Yasuhiro Nakazawa,[c] Wolfgang Wernsdorfer,[d] Ken-ichi Sugiura,[a] Masahiro Yamashita,[e] Claude Coulon,[f] and Rodolphe Clérac*[f]

Abstract: An alternated 1:1 chain compound of a Mn^{III} salen derivative and the TCNQ monoradical was synthesized: [Mn(5-TMAMsaltmen)(TCNQ)]$(ClO_4)_2$ (**1**) (TCNQ = tetracyano-*p*-quinodimethane; 5-TMAMsaltmen = *N*,*N*′-(1,1,2,2-tetramethylethylene) bis(5-trimethylammoniomethylsalicylideneiminato)). Compound **1** has a zigzag chain structure packed with adjacent chains with an interchain Mn···Mn distance of over 8 Å. As compound **1** contains no crystallization solvent, the void spaces between chains are occupied only by ClO_4^- counter ions. Compound **1** has a structure reminiscent of what has been observed in the family of Mn^{III}(porphyrin)-TCNE or -TCNQ compounds reported previously by Miller and co-workers and we demonstrate herein its unique single-chain magnet behavior among this family of compounds. The direct current (dc) magnetic measurements established the one-dimensional nature of compound **1** with an antiferromagnetic exchange coupling, $J/k_B \approx -96$ K, between the Mn^{III} ion and TCNQ radical and with an activated correlation length ($\Delta_\xi = 26.5$ K) at low temperatures (50–15 K). The slow relaxation of the magnetization was shown in compound **1** by the field hysteresis of the magnetization observed below 3.5 K (with a coercive field up to 14 kOe at 1.8 K). Single-crystal magnetization measurements demonstrated the uniaxial symmetry of this compound and allowed an estimation of the anisotropy field, $H_a \approx 97$ kOe. The absence of magnetic ordered phase or spin-glass behavior was established by heat-capacity calorimetry measurements that exhibit no abnormality of C_p between 0.5 K and 10 K. The study of the magnetization relaxation by combined ac (alternating current) and dc techniques showed that compound **1** possesses a single relaxation time (τ). As the consequence of the finite size of the chain, the temperature dependence of τ presents two activated regimes above and below 4.5 K with $\tau_{01} = 2.1 \times 10^{-10}$ s, $\Delta_{\tau 1} = 94.1$ K and $\tau_{02} = 6.8 \times 10^{-8}$ s and $\Delta_{\tau 2} = 67.7$ K, respectively. The detailed analysis of these dynamics properties together with the correlation length, allows an unambiguous demonstration of the single-chain magnet behavior in **1**.

Keywords: magnetic properties · manganese · salen-type ligand · single-chain magnet · TCNQ

[a] Prof. H. Miyasaka, T. Madanbashi, Prof. K.-i. Sugiura
Department of Chemistry, Graduate School of Science
Tokyo Metropolitan University, 1-1 Minami-ohsawa
Hachioji, Tokyo 192-0397 (Japan)
and
CREST, Japan Science and Technology Agency (JST)
4-1-8 Honcho, Kawaguchi, Saitama 332-0012 (Japan)
E-mail: miyasaka@agnus.chem.tohoku.ac.jp

[b] Dr. K. Sugimoto
X-Ray Research Laboratory, Rigaku Co. Ltd.
3-9-12 Matsubara-cho, Akishima, Tokyo 196-8666 (Japan)

[c] Prof. Y. Nakazawa
Department of Chemistry, Graduate School of Science
Osaka University, Machikaneyama 1-1
Toyonaka, Osaka 560-0043 (Japan)

[d] Dr. W. Wernsdorfer
Laboratoire Louis Néel, CNRS, BP 166
25 Avenue des Martyrs, 38042 Grenoble Cedex 9 (France)

[e] Prof. M. Yamashita
Department of Chemifstry, Graduate School of Science
Tohoku University, Aramaki-Aza-Aoba, Aoba-ku
Sendai, 980-8578 (Japan)
and
CREST, JST, 4-1-8 Honcho, Kawaguchi, Saitama 332-0012 (Japan)

[f] Prof. C. Coulon, Dr. R. Clérac
Centre de Recherche Paul Pascal, CNRS UPR 8641
115 Avenue du Dr. A. Schweitzer, 33600 Pessac (France)
Fax: (+33) 556-845-600
E-mail: clerac@crpp-bordeaux.cnrs.fr

[g] Prof. H. Miyasaka
Current address: Department of Chemistry
Graduate School of Science, Tohoku University
Aramaki-Aza-Aoba, Aoba-ku, Sendai 980-8578 (Japan)
Fax: (+81) 22-795-6548

[**] TCNQ = tetracyano-*p*-quinodimethane.

Introduction

The development of one-dimensional (1D) systems towards creating new magnetic materials has been extensively conducted over the past two decades. However, the experimental evidence of "single-chain magnet" (SCM) behavior was only discovered at the beginning of this century,[1–7] although the slow dynamics of the magnetization in the ferromagnetic Ising chain was predicted by R. J. Glauber back in 1963.[8] While the slow relaxation of the magnetization observed in single-molecule magnets (SMMs)[9] is solely induced by the high-spin ground state (S_T) and its uniaxial anisotropy ($D<0$ and small E) of the targeted polynuclear complex,[10] the "magnet"-type behavior observed in SCMs is an intrinsic magnetic property of an isolated chain composed of anisotropic high-spin (S_T) units linked in a one-dimensional (1D) manner by significant intrachain exchange interaction (J).[2] Both types of "magnet" are indeed superparamagnetic systems that display slow relaxation of their magnetization. The global magnetization of these materials relaxes to zero with a characteristic time (τ). With lowering temperature, this time is activated and becomes longer and longer and finally reaches the characteristic time of the experiment (τ_{exp}) where it becomes experimentally detectable. This crossover ($\tau_{exp}=\tau$) is thus achieved at a blocking temperature (T_B). At lower temperatures ($T \ll T_B$), τ can be of the order of years and the material can be therefore considered as a "magnet". Thus, these materials should be distinguished from classical magnets that exhibit a long-range magnetic order.

In the past fifteen years, Miller and co-workers have reported extensively on a family of alternated chains composed of ferrimagnetically arranged Mn^{III} porphyrin derivatives ($S_{Mn}=2$) and organic radicals ($S_{rad}=1/2$) such as $TCNE^{\bullet-}$ (tetracyanoethenide),[11] $TCNQ^{\bullet-}$ (tetracyano-*p*-quinodimethanide),[12] and their related molecules (hexacyanobutadiene,[13] tetrachloro-1,4-benzoquinonide,[14] *N*,*N*′-dicyanoquinonediimine[15]). Interestingly, among these materials, some of them exhibit "magnet"-type behavior with original slow relaxation of the magnetization that has been interpreted in the frame of a Spin-Glass (SG) description (quasi-1D fractal cluster glass model).[16] Epstein and co-workers have elucidated the key role of the dipolar interactions between chains to explain the magnetic viscous behavior observed for an example in [Mn(tpp)(TCNE)]·2(1,3-$C_6H_4Cl_2$) (tpp = *meso*-tetraphenylporphyrin).[16,17] In these materials, the observed slow relaxation would not be thus induced by isolated chains as in SCM systems, but by the introduction of magnetic correlation between chains.

Herein we report on a new Mn^{III}/TCNQ member of this family that displays unambiguous evidence of SCM behavior. The newly synthesized material, [Mn(5-TMAMsaltmen)(TCNQ)](ClO_4)$_2$ (**1**) (5-TMAMsaltmen is a tetradentate neutral ligand of *N*,*N*′-(1,1,2,2-tetramethylethylene) bis(5-trimethylammoniomethylsalicylideneiminato)) made of a Mn^{III} salen derivative unit and the TCNQ radical, that exhibits the ferrimagnetic alternated chain topology observed in Miller's compounds. While many of Miller's compounds and in particular [Mn(tpp)(TCNE)]·x(1,3-$C_6H_4Cl_2$) possess removable interstitial solvents that considerably affect the magnetic properties due to disorder effects (for example, the blocking temperature ranged from 7.8 to 11.3 K depending on the interstitial solvent contents),[16] compound **1** has no crystallization solvent in its crystal unit cell. This remarkable feature induces a high stability in compound **1** and allowed us to study its intrinsic magnetic properties that have arisen from a single Mn^{III}/TCNQ chain and its "fixed" packing arrangement.

Results and Discussion

General properties: Compound **1** was synthesized as fine purplish-brown crystals by the assembly reaction of [Mn(5-TMAMsaltmen)(H_2O)$_2$](ClO_4)$_3$ with Li(TCNQ) in a solution of acetonitrile/methanol (Scheme 1). It should be emphasized that crystals of compound **1** are very stable in the experimental atmosphere after removal of the mother liquid, as the physical characterizations (by IR spectroscopy, X-ray diffraction, and magnetic properties) stay unchanged over a few months. The IR spectroscopy study on **1** shows significant low-energy ν(C≡N) vibrations at 2189(s) and 2127(s) cm^{-1}. These bands can be attributed to the monoradical $TCNQ^{\bullet-}$ form consistently with the vibration bands at 2197 and 2168 cm^{-1} for Li(TCNQ) or at 2197 and 2166 cm^{-1} for Na(TCNQ),[18] while neutral TCNQ or diradical $TCNQ^{2-}$ are observed at 2200 cm^{-1}, and 2164 and 2096 cm^{-1} (Na_2TCNQ),[17] respectively. In agreement with the structural description (vide infra), the observation of two separated absorption bands in the spectrum for compound **1** reveals the presence of both coordinated and non-coordinated C≡N groups on the TCNQ monoradicals.

Structural description: Compound **1** crystallizes in the monoclinic space group $C2/c$ ($Z=4$). An ORTEP drawing of the asymmetrical unit is depicted in Figure 1a and selected bond lengths and angles are listed in Table 1. The repeating unit consists of the [Mn(5-TMAMsaltmen)] moiety and the TCNQ radical in a 1:1 stoichiometry with the Mn atom located on a special site 4*e* (C_2 symmetry; 0, *y*, 1/4) and an inversion center at the midpoint of the TCNQ molecule. The coordination sphere around the Mn ion is an elongated octahedron with the 5-TMAMsaltmen tetradentate ligand surrounding the manganese equatorial plane with bond lengths of Mn(1)–O(1) = 1.885(2) and Mn(1)–N(1) = 1.980(2) Å. On the other hand, the two left Mn axial positions are occupied by nitrogen atoms of the TCNQ molecule (*trans–anti*-fashion of TCNQ) with Mn(1)–N(3) = 2.380(4) Å. The Mn(1)-N(3)-C(15) angle and dihedral angle made by the TCNQ and Mn(5-TMAMsaltmen) equatorial planes in compound **1** are found to be 123.8(3) and 40.3° respectively. The axial distortion of the Mn octahedron coordination sphere corresponds to a Jahn–Teller axis typically observed for Mn^{III} salen analogues (N(3)-Mn(1)-N(3)* = 168.6(1)°; symmetry operation *, $-x+2$, y, $-z+1/2$). It is

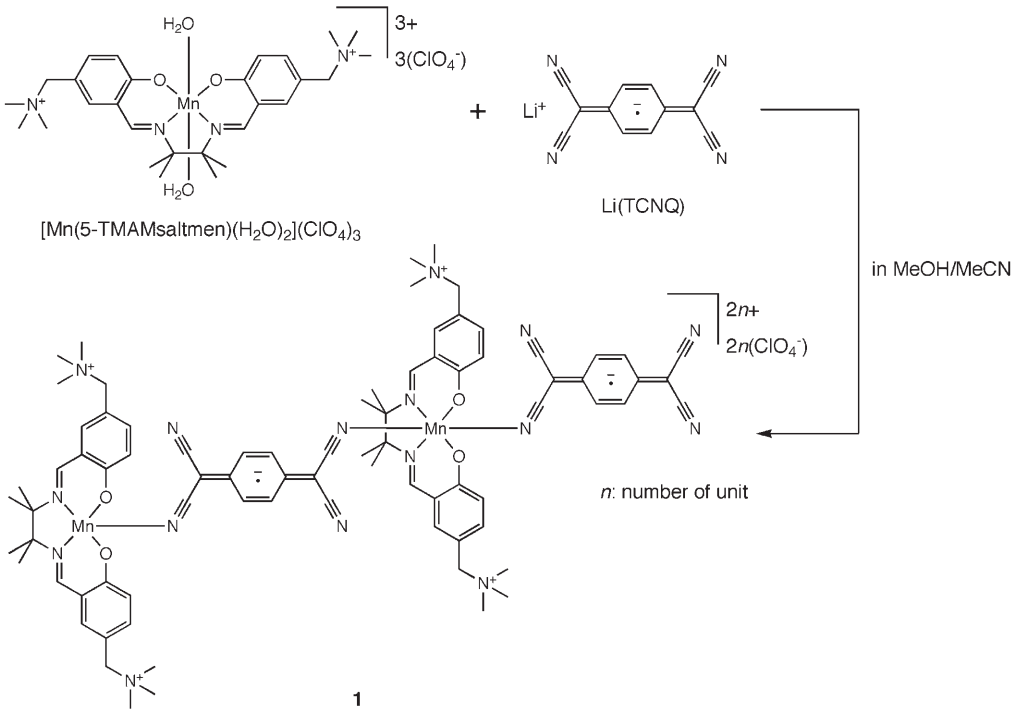

Scheme 1.

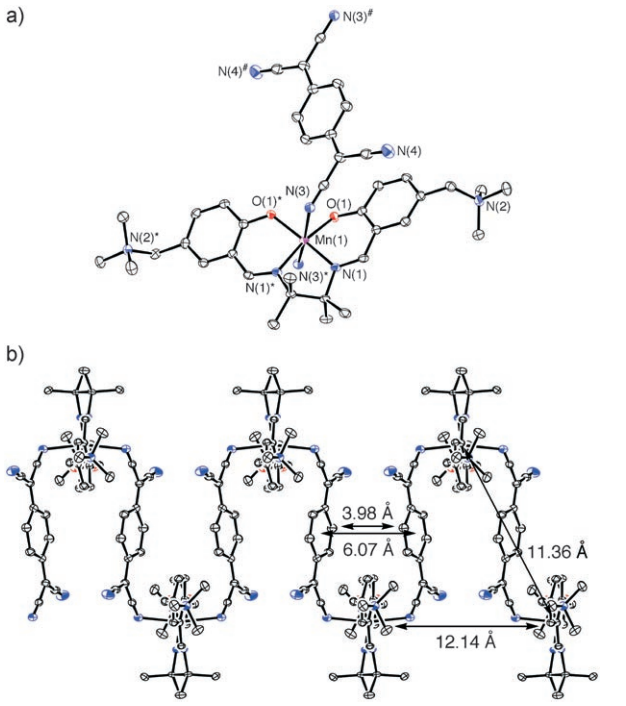

Figure 1. ORTEP drawings of: a) The repeating unit and; b) the zigzag chain structure in **1** (thermal ellipsoids drawn at 50% probability). Hydrogen atoms and perchlorate anions were omitted for clarity. The intrachain Mn···Mn distances through the TCNQ moiety or along the *c* direction are 11.36 and 12.14 Å, respectively. Between neighboring TCNQ radicals, the nearest C···C distance is C(19)···C(19) = 3.98 Å and the midpoint-to-midpoint distance is 6.07 Å.

Table 1. Bond lengths and angles of [Mn(5-TMAMsaltmen)(TCNQ)]-$(ClO_4)_2$ (**1**) with the estimated standard deviations in parentheses.

	Bond length [Å]		Bond angle [°]
Mn(1)–O(1)	1.885(2)	N(1)-Mn(1)-O(1)	92.06(9)
Mn(1)–N(1)	1.980(2)	N(3)-Mn(1)-O(1)	88.5(1)
Mn(1)–N(3)	2.380(4)	N(3)-Mn(1)-N(1)	88.0(1)
N(3)–C(15)	1.153(4)	N(3)-Mn(1)-N(3)[b]	168.6(1)
N(4)–C(17)	1.141(5)	N(3)-Mn(1)-O(1)[b]	83.9(1)
C(15)–C(16)	1.413(4)	N(3)-Mn(1)-N(1)[b]	100.7(1)
C(16)–C(17)	1.422(5)	N(1)-Mn(1)-N(1)[b]	81.5(1)
C(16)–C(18)	1.431(5)	O(1)-Mn(1)-O(1)[b]	95.80(9)
C(18)–C(19)	1.419(5)	Mn(1)-N(3)-C(15)	123.8(3)
C(19)–C(20)	1.370(5)		
C(18)–C(20)[a]	1.421(5)		
Mn(1)–Mn(1)[a]	11.3583(7)		

[a] Symmetry operators: $-x+2$, $-y+1$, $-z+1$. [b] Symmetry operators: $-x+2$, y, $-z+1/2$.

worth noting that the Jahn–Teller axes are all parallel in the chain arrangement and oriented at about 14° from the *c* axis or chain direction in the *ac* plane. In order to discuss the magnetic properties of compound **1** in the next part of this paper, the oxidation state of the Mn ion and TCNQ moiety must be established without ambiguity. The oxidation state of the Mn ions is clearly trivalent from the characteristic coordination geometry (Jahn–Teller distortion) as previously mentioned. For the TCNQ moieties, the results from the IR spectroscopy described above suggest the presence of a monoradical. A detailed analysis of TCNQ bond lengths is

also a useful tool to probe the degree of reduction of this type of redox molecule. Indeed, while the C≡N bond length is mainly affected by the Mn–N coordination, the C–C distances in the TCNQ molecule are good indicators of the oxidation state. The degree of charge on the TCNQ moiety has been thus estimated by Kistenmacher and co-workers from the empirical relationship: $\rho = A[c/(b+d)] + B$,[19] where $A = -41.667$ and $B = 19.833$ have been determined from the neutral TCNQ[20] and monoradical form in Rb(TCNQ)[21] ($\rho = 0$ and -1, respectively), and the b~d parameters have been defined as shown by the scheme included in Table 2. Since the TCNQ moiety in compound **1** has an inversion center at its midpoint, two kinds of bond sets (for a coordinated and non-coordinated site) can be considered as listed in Table 2. In agreement with the IR data, the TCNQ charge in compound **1** estimated from the Kistenmacher relation is about -1.2, confirming the monoanionic nature of TCNQ.

As shown in Figure 1b, the $TCNQ^{\bullet-}$ moiety coordinates to $[Mn(5\text{-TMAMsaltmen})]^{3+}$ in a *trans–anti*-coordination fashion to form an alternated zigzag chain. The intrachain Mn···Mn distances through the TCNQ moiety (neighbor distance) or along the *c* direction (next-neighbor distance) are 11.3583(7) and 12.14 Å, respectively. The packing arrangement of chains of compound **1** is shown in Figure 2. The chains are running along the *c* axis, where the nearest interchain Mn···Mn distances are 8.35 and 11.53 Å between the neighboring chains along the *b* axis and the *a* axis directions, respectively. As seen in Figure 2b, the TCNQ moieties form a one-dimensional column along the *c* axis. However, as the TCNQ moieties are alternately sliding along the *c* axis with the tilt angle of 20°, there is no significant π–π interactions between neighboring TCNQ radicals (Figure 2), (the nearest C···C distance is C(19)···C(19) = 3.977(6) Å and the midpoint-to-midpoint distance is 6.07 Å (Figure 1b)). The perchlorates as counter-anions are located between chains in the void space left available between the bulky 5-TMAMsaltmen ligands. It is worth noting at this stage that after a careful analysis of the packing arrangement, no interchain π–π stacking has been identified.

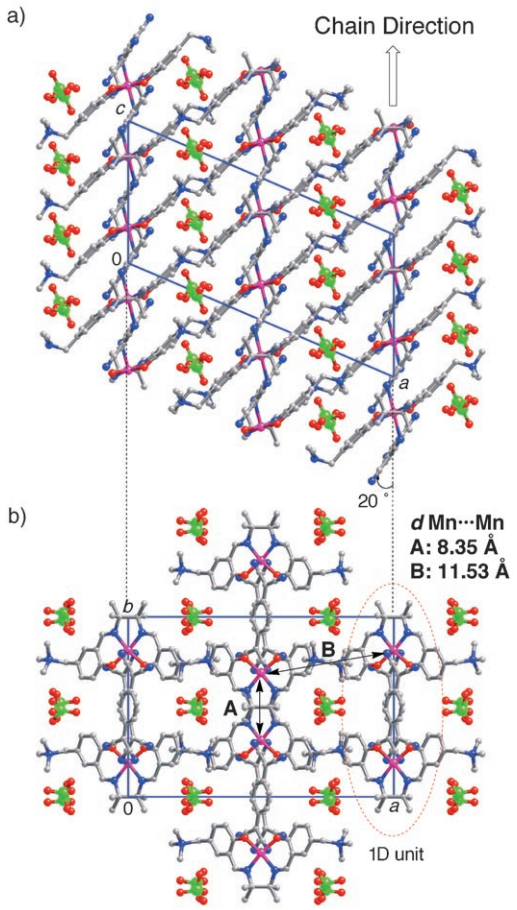

Figure 2. Packing arrangements of **1** showing: a) The projection along the *b* axis and; b) the projection along the *c* axis. The moiety bounded by a red dotted circle forms a chain.

dc magnetic studies: The dc magnetic susceptibility (χ) was measured in the temperature range of 1.8 to 300 K at an applied field of 1 kOe on a polycrystalline sample of compound **1** restrained by using *n*-eicosane. The χT versus T plot is shown in Figure 3a. The χT value of 2.51 $cm^3 K mol^{-1}$

Table 2. Summary of bond lengths [Å] in the TCNQ moiety and estimated charge.

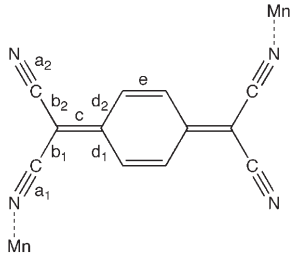

Compound	a	b	c	d	e	b+d	c/(b+d)	ρ[a]	Ref.
TCNQ	1.140(1)	1.441(4)	1.374(3)	1.448(4)	1.346(3)	2.889	0.476	0	[19]
Rb(TCNQ)	1.153(7)	1.416(8)	1.420(1)	1.423(3)	1.373(1)	2.839	0.500	−1	[20]
1 (coordination site)	1.153(4) [a_1]	1.413(4) [b_1]	1.431(5)	1.421(5) [d_1]	1.370(5)	2.834	0.505	−1.21	this work
1 (non-coordination site)	1.141(5) [a_2]	1.422(5) [b_2]	1.431(5)	1.419(5) [d_2]	1.370(5)	2.841	0.504	−1.15	this work

[a] $\rho = A[c/(b+d)] + B$, where $A = -41.667$ and $B = 19.833$ were determined assuming that neutral TCNQ and Rb(TCNQ) correspond to $\rho = 0$ and -1, respectively.

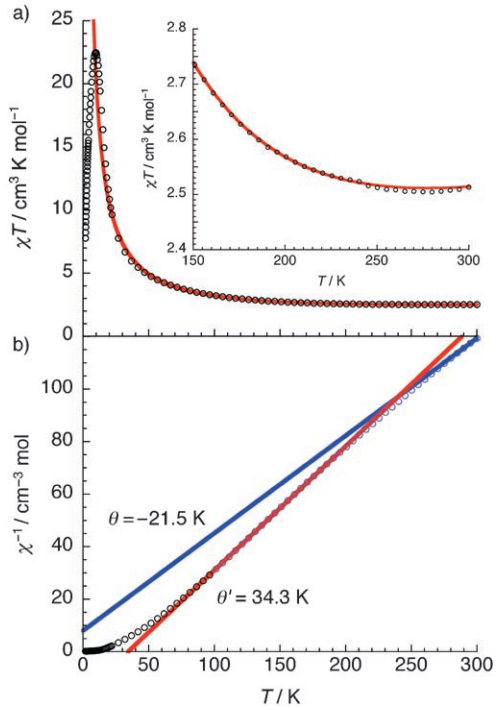

Figure 3. Temperature dependence of: a) χT and; b) χ^{-1} measured on a polycrystalline sample of **1** at 1 kOe. In the χT versus T plot, the red line represents a good simulation by using the Seiden model with $S_{Mn}=2$ and $s_{Rad}=1/2$ (see text). In the χ^{-1} versus T plot the blue and red lines represent linear fits of the data above and below 270 K, respectively.

at 300 K is smaller than the predicated value of 3.375 $cm^3 K mol^{-1}$ for isolated $S_{Mn}=2$ and $s_{Rad}=1/2$ spins. With decreasing temperature from 300 K, the χT product, initially, slightly decreases and gives a broad minimum at approximately 270 K (inset of Figure 3a). From this minimum, the χT product increases to reach a maximum of 22.5 $cm^3 K mol^{-1}$ at about 10 K. Below the maximum, the χT product abruptly decreases to 7.8 $cm^3 K mol^{-1}$ at 1.8 K. This type of behavior, including a high-temperature broad minimum followed by a steep increase, suggests that strong antiferromagnetic couplings are operative between the Mn^{III} ion ($S_{Mn}=2$) and $TCNQ^{\bullet -}$ ($s_{Rad}=1/2$). As generally applied to the Mn^{III}(porphyrin)–TCNE or -TCNQ systems by Miller and co-workers, the magnitude of magnetic coupling between the two magnetic centers has been determined by fitting the susceptibility data to an alternating chain model of quantum spins, s_i, and classical spins S_i (also called the Seiden model) considering the following spin Hamiltonian:[22]

$$H = -2J \sum_{i=1}^{N} (\vec{S}_{Mn,i} + \vec{S}_{Mn,i+1}) \cdot \vec{s}_{Rad,i} \qquad (1)$$

Between 30 and 300 K, the best least-squares fit yields $g_{Mn}=1.91$, $g_{rad}=2.00$, $J/k_B=-96.1$ K (red solid line in Figure 3a). Consequently, compound **1** is made of strongly antiferromagnetically coupled $S_{Mn}=2$:$s_{Rad}=1/2$ spin chains forming a ferrimagnetic one-dimensional arrangement.

Considering the existence of the χT minimum around 270 K, the Curie–Weiss fit should be done above this temperature. The least-squares linear fitting above 270 K roughly yielded a Weiss constant (θ) of about −21 K (blue line in Figure 3b), such a large negative value being consistent with the J value found by the fitting of the experimental χT product (see above). Another effective Weiss constant, θ', evaluated below the rounded minimum of χT, has been used extensively by Miller and co-workers as a phenomenological probe to correlate the intrachain interaction and structural parameters in many compounds based on Mn^{III}(porphyrin)–TCNE or -TCNQ.[11,12] The exchange coupling between Mn^{III} ion and TCNQ or TCNE radical anions in these types of materials is strongly influenced by two intimately related angles: the coordination angle (Mn−N≡C) and the dihedral angle between the radical mean plane and Mn^{III} equatorial plane (note that small Mn−N≡C angles usually correspond to small dihedral angles).[23] Those angles are indeed governing the overlap between the d_{z^2} orbital on the Mn^{III} ion and the pπ orbital on the coordinating nitrogen atom of the radical moiety. In other words, a large overlap allows stronger antiferromagnetic coupling and thus a larger θ' value. Indeed, a linear variation of θ' versus the dihedral angle is obtained (Figure 4a) for compound **1** together with a series of Mn^{III}(porphyrin)–TCNE or -TCNQ compounds reported by Miller and co-workers (Table 3). For compound **1**, the θ' value has been evaluated at about 34 K in the middle temperature range of about 100–200 K (red line in Figure 3b). Figure 4b is a plot of the J value estimated by the Seiden model versus the dihedral angle, and as well as in Figure 4a, a linear relation is observed, confirming indirectly the J value for compound **1** in the series of Mn^{III}/TCNQ, TCNE materials. Interestingly, as far as we know, only two other one-dimensional assemblies of Mn^{III} complexes with the TCNQ radical have been described so far.[11] Compound **1** has the smallest dihedral and Mn-N≡C angles allowing the best d_{z^2}/pπ orbital overlap and thus the largest θ' (and J) value of this family of Mn^{III}/TCNQ materials (Figure 4). Thus, compound **1** belongs to two related one-dimensional families of compounds, the Mn^{III}/TCNE and Mn^{III}/TCNQ materials, in which high-temperature magnetic properties are dominated by the intrachain interactions.

For compound **1**, the intrachain interaction (J) is thus clearly dominating as shown by the analysis of the temperature dependence of the χT product above 30 K (vide supra). Below 30 K, the one-dimensional nature of compound **1** can also be checked following the correlation length of the system that is proportional to the χT product at zero dc field in any one-dimensional classical problem. In a ferro- or ferrimagnetic one-dimensional system described in the frame of an anisotropic Heisenberg model, this correlation length exponentially increases on decreasing the temperature, and $\chi T = C_{eff} \exp(\Delta_\xi/T)$.[24,25] According to K. Nakamura and co-workers, the corresponding gap, Δ_ξ, is the energy necessary to create a domain wall in the chain.[25,26] In the Ising limit ($|D| \gg 4|J|/3$),[27] this energy can be simply expressed as $\Delta_\xi = 4JS_T^2$, but its expression becomes nonana-

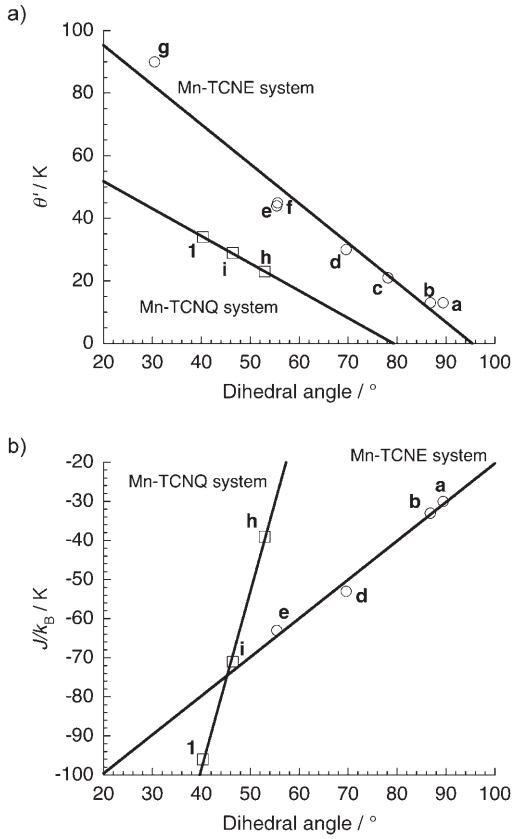

Figure 4. Correlation between the dihedral angle defined by the MnN_4 or MnO_2N_2 plane and the $TCNE^{\bullet-}$ or $TCNQ^{\bullet-}$ plane, and the effective θ' value (a) and the exchange coupling J obtained by using the Seiden model (b) (see text). Compounds **a** to **i** are Mn^{III} porphyrin systems listed in Table 3 and reported by J. S. Miller and co-workers.

lytical in more complicated situations such as ferrimagnetic arrangements, quantum spins, mixed classical-quantum spins, $|D| \leq 4|J|/3$... Figure 5 shows the plot of $\ln(\chi' T)$ versus $1/T$, where χ' is zero-field susceptibility deduced from complementary dc and ac measurements. As expected for anisotropic one-dimensional systems, the $\ln(\chi' T)$ term in-

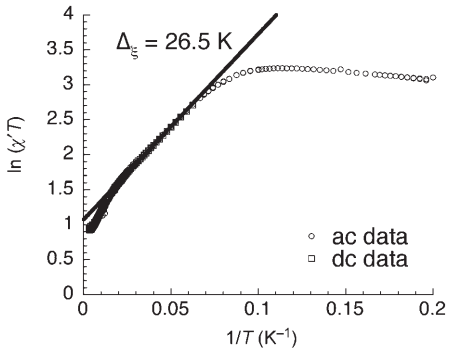

Figure 5. Plot of $\ln(\chi' T)$ versus $1/T$ for compound **1**, where square and circle symbols have been obtained with dc (1 kOe dc field) and ac (1 Hz ac frequency, 3 Oe ac field and zero dc field) techniques, respectively.

creases linearly with the inverse of the temperature between 50 and 15 K; the energy gap, Δ_ξ, is 26.5 K and C_{eff} is 1.07 $cm^3 K mol^{-1}$. It is noteworthy that this effective Curie constant is in excellent agreement with the expected value for an Ising $S_T = 3/2$ ($S_T = S_{Mn} - s_{Rad}$) spin: $C_{Ising} = Ng^2\mu_B{}^2 S_T{}^2/(3k_B) = 1.125\ cm^3 K mol^{-1}$. As mentioned above, the ferrimagnetic arrangement with the presence of $s = 1/2$ quantum spins in the chain and the presence of magnetic anisotropy only in the Mn^{III} sites complicate the determination of the correlation length, its theoretical expression, and thus the analysis of Δ_ξ. However, the exponential increase of the $\chi' T$ product above 10 K clearly establishes the 1D nature of compound **1**. At 10 K, the value of $\ln(\chi' T)$ goes through a maximum and a slow linear decrease is observed at lower temperatures. This type of behavior is usually observed when the correlation length becomes larger than the average distance between two intrinsic defects along the chain as already observed in a few SCM systems.[2c,f,1d,5d] Nevertheless, this phenomenon occurs here at 10 K, while this finite-sized crossover occurs unequivocally at 4.5 K on the relaxation time scale (vide infra). This discrepancy concerning the crossover temperature implies the presence of another effect that dramatically modifies the growth of the

Table 3. Bond lengths, angles, and several magnetic parameters for Mn^{III} porphyrin/TCNQ or/TCNE assemblies and for **1**.

Compound	Mn–N [Å]	Mn-N-C [°]	Dihedral angle [°][a]	Intrachain Mn···Mn [Å][b]	θ' [K][c]	T_{min} [K][d]	J/k_B [K][e]	Ref.
TCNE system								
[Mn(TBrPP)(TCNE)]·2MePh (**a**)	2.293	168.1	89.4	10.277	13	80	−30	[11l]
[Mn(TClPP)(TCNE)]·2MePh (**b**)	2.267	167.2	86.8	10.189	13	110	−33	[11i,j]
[Mn(TOMePP)(TCNE)]·2MePh (**c**)	2.289	165.5	78.1	10.256	21	134		[11i,k]
[Mn(TIPP)(TCNE)]·2MePh (**d**)	2.276	158.7	69.6	10.101	30	160	−53	[11l]
[Mn(TPP)(TCNE)]·2MePh (**e**)	2.305 (av)	147.9 (av)	55.4 (av)	10.116	44	191	−63	[11i,g,17]
[Mn(TFPP)(TCNE)]·2MePh (**f**)	2.309	150.3	55.6	10.185	45	240		[11i,k]
[Mn(TP′P)(TCNE)]·2MePh (**g**)	2.299	129	30.4	8.587	90	>300		[11b,i]
TCNQ system								
[Mn(TMesP)(DMTCNQ)]·2*p*-Me_2Ph (**h**)	2.332 (av)	142.2 (av)	52.9 (av)	11.43	23	115	−39	[12a]
[Mn(T(MeO)$_3$PP)(TCNQF$_4$)]·3*o*-Cl_2Ph (**i**)	2.321	135.9	46.4	12.685	29	215	−71	[12b]
[Mn(5-TMAMsaltmen)(TCNQ)](ClO_4)$_2$ (**1**)	2.380	123.8	40.3	11.358	34	270	−96	this work

[a] The angle is defined by the dihedral angle made by the TCNE (or TCNQ) plane and the Mn^{III}(tetradentate ligand) equatorial plane. [b] This distance is through the TCNE or TCNQ moiety. [c] Effective θ' value (see text). [d] Temperature indicating the χT minimum. [e] From the fitting by the Seiden model (see text).

correlation length. As shown in $[Mn_2(saltmen)_2Ni(pao)_2(py)_2](ClO_4)_2$ ($saltmen^{2-}$: *N*,*N*′-(1,1,2,2-tetramethylethylene) bis(salicylideneiminate), pao^-: pyridine-2-aldoximate, py: pyridine), the presence of weak interchain interactions has been invoked to explain such behavior.[2d]

The field dependence of the magnetization was measured on a polycrystalline sample of compound **1** in the temperature range 1.8–4 K (Figure 6). Compound **1** displays slow relaxation of the magnetization, as shown by the field hysteresis loops observed below 3.5 K with a coercive field reaching 14 kOe at 1.8 K. At high fields above 20 kOe, a linear increase of the magnetization is observed, as generally seen in anisotropic systems. To determine H_a, the anisotropy field (roughly estimated to be 100 kOe from the polycrystalline sample data shown in Figure 6), we have performed high-field single-crystal measurements by using Hall probe techniques. The easy axis of the crystal was found at about 15° from the chain direction (*c* axis) in the *ac* plane corresponding to the Jahn–Teller direction of the Mn^{III} metal ions. The plane perpendicular to the easy axis is almost isotropic, as expected for a uniaxial anisotropy, and can be therefore considered as a hard plane. In this plane, the field dependence of the magnetization has been measured up to 140 kOe (Figure 7). At 1.5 K, the magnetization increases linearly and saturates at around 97 kOe (H_a). To link H_a to the magnetic anisotropy, a phenomenological approach considering a chain of effective $S_T = 3/2$ classical spins can be used at low temperature when the exchange energy is much larger than any other energy scale of the system. In this limit, the magnetization, which is determined for when the field is applied perpendicularly to the easy axis, is obtained by minimizing the effective energy: $E_{eff} = K\sin^2(\theta) - g\mu_B H S_T \sin(\theta)$ (where K is a phenomenological anisotropy parameter and θ the angle between the effective spins and the easy axis). The resulting equilibrium magnetization is $M = g\mu_B S_T \sin(\theta_{min})$.[28] The saturation of the magnetization is obtained for $\sin(\theta_{min}) = 1$, which leads to $2K = g\mu_B S_T H_a$ and thus $K/k_B = 9.8$ K. Considering that the magnetic anisotropy definitely originates solely from the single-ion anisotropy of the $S = 2$ Mn^{III} site, K can be rewritten as $-D_{Mn}S_{Mn}^2$. Therefore, one can easily deduce that $D_{Mn}/k_B = -2.4$ K is in good agreement with the values obtained for similar Mn^{III} building blocks.[2d,g,29]

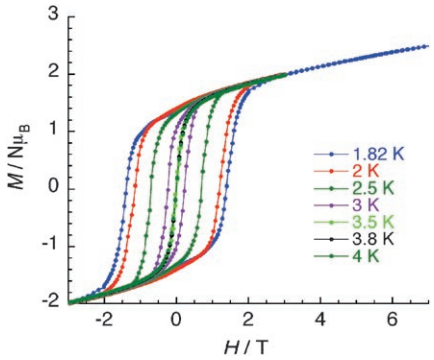

Figure 6. Field dependence of the magnetization on a polycrystalline sample of **1** at different temperatures at and below 4 K.

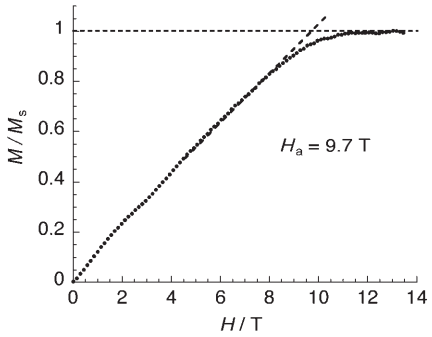

Figure 7. Field dependence of the normalized magnetization (M/M_S where M_s is the magnetization at saturation at 14 T) on a single crystal of **1** oriented in the hard plane perpendicular to the easy axis of the magnetization at 1.5 K with a sweep-field rate of 0.035 T s^{-1}.

Single-crystal heat-capacity measurements: The heat capacity of compound **1** was measured on a single crystal in the temperature range 0.6–10 K under an applied dc field of 0, 0.5, 1, and 4 T. Figure 8 shows the experimental results plotted as C_p/T versus T. No anomaly was observed regardless of the applied field over the entire temperature range measured. This result indicates unambiguously the absence of long-range magnetic order or spin-glass-like behavior in this system despite the observation of field hysteresis of the magnetization. This result agrees with what is typically seen in superparamagnetic materials such as SMMs[30] or SCMs.[31]

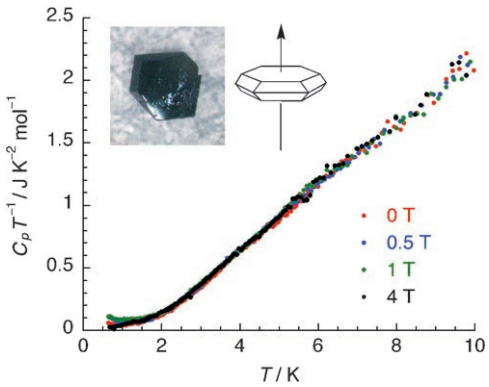

Figure 8. Plots of C_pT^{-1} versus T for **1** measured on a single crystal under zero and several applied fields.

Study of the relaxation time: The frequency dependence of ac susceptibilities was measured in the temperature range 1.8–12 K under an oscillating magnetic field of 3 Oe and zero dc field (Figure 9). Below 10 K, in-phase (χ') and out-of-phase (χ'') ac susceptibilities are found to be strongly de-

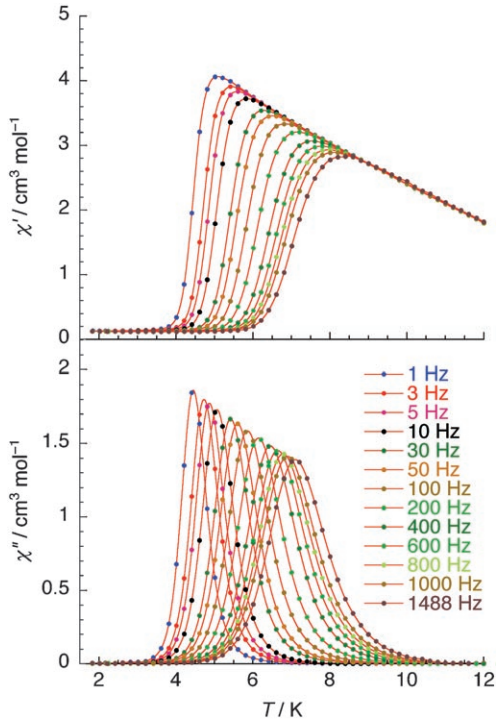

Figure 9. Temperature dependence of the ac susceptibilities for **1** measured at several ac frequencies, where χ' and χ'' are in-phase and out-of-phase susceptibilities, respectively. The solid lines are guides for the eye.

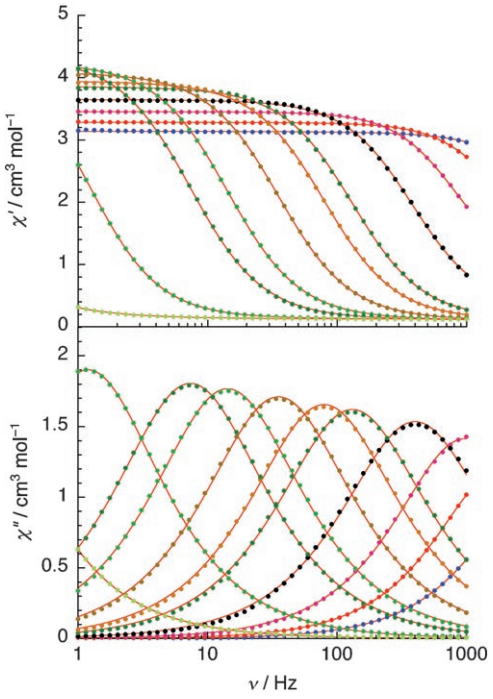

Figure 10. Frequency dependence of the ac susceptibilities for **1** measured between 4 and 8 K. The solid red lines are the best fits obtained with the generalized Debye model ($\alpha < 0.1$).

pendent on the frequency. In line with the static magnetic data and heat-capacity measurements, this result rules out the possibility of a three-dimensional long-range order and spin-glass-like behavior. As already mentioned for the M versus H data, this frequency-dependent ac susceptibility indicates the slow relaxation of the magnetization as observed for SMMs or SCMs. Considering the chain arrangement of compound **1** and its one-dimensional magnetism (vide supra), the present magnetization dynamics indicate the occurrence of SCM behavior. At a given frequency (ν), the energy input to the system by the thermal bath is not enough to let the magnetization (M) follow the applied oscillating field, which hence becomes frozen below the so-called blocking temperature $T_B(\nu)$. This blocking process causes the ac response to decrease completely in parallel to the increase of coercivity. To study and determine the relaxation time of the system, additional ac susceptibility measurements as a function of ac frequency (ν) have been performed at fixed temperatures between 4 and 8 K (Figure 10). The data have been simulated by using a generalized Debye model taking into account a distribution of relaxation quantified by the α parameter (ranging from 0 to 1, note that $\alpha = 0$ indicates the presence of a unique relaxation time: a Debye mode).[32] In the entire temperature range measured, the α parameter was always found to be less than 0.1, indicating a very narrow distribution of relaxation times. Therefore in a good approximation, compound **1** has a single relaxation time (note that this result also excludes the spin-glass interpretation). Cole–Cole diagrams (χ'' versus χ' plot shown in Figure 11) also illustrate nicely the presence of only one relaxation process as they exhibit systematically a quasi-semicircle shape that can be perfectly fitted to the generalized Debye model with $\alpha < 0.1$.

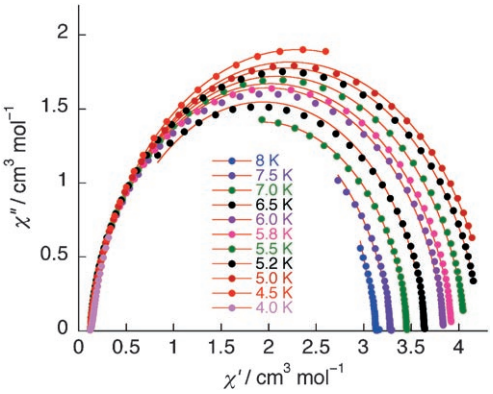

Figure 11. Cole–Cole plots for **1**. The solid red curves represent the least-squares fit to a generalized Debye model with $\alpha < 0.1$.

In such a single relaxation process, τ can be deduced from the previous fits and also from the $\chi''(T)$ plots (Figure 9) considering that at a given frequency (ν), the peak of $\chi''(T)$ is located at the blocking temperature, where $\tau(T_B) = 1/(2\pi\nu)$. As demonstrated by Glauber in 1963,[8] SCMs possess

a thermally activated relaxation time (Arrhenius law, [Eq. (2)]):

$$\tau(T) = \tau_0 \exp\left(\frac{\Delta_\tau}{T}\right) \quad (2)$$

where τ_0 is a pre-exponential factor, and Δ_τ is an energy barrier quantifying the magnetization reversal. The semilog plot of τ versus T^{-1} by using ac data (blue dots in Figure 12)

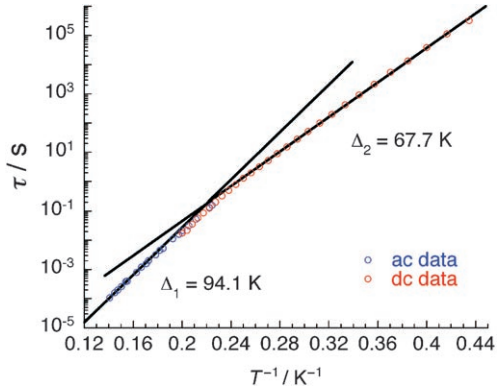

Figure 12. Relaxation time (τ) versus $1/T$ plot for **1**, where blue and red dots were obtained from ac and dc measurements, respectively.

confirms this prediction with $\tau_{01} = 2.1 \times 10^{-10}$ s, $\Delta_{\tau 1} = 94.1$ K. With our commercial SQUID apparatus, this relaxation time cannot be followed below 4 K and 1 Hz. Therefore, magnetization decay measurements have been performed on a home-made micro-SQUID magnetometer to access lower temperatures. It is worth noting that below 2 K, the relaxation process becomes too slow and the estimation of the relaxation time becomes impossible even with the micro-SQUID apparatus. The obtained τ values have been plotted in Figure 12 (red dots) together with those derived from the ac magnetic measurements. Above $T^* = 4.5$ K ($1/T^* = 0.22$ K^{-1}), the relaxation times deduced from the dc measurements are in agreement with the ac data. The fits of the complete set of data above 4.8 K led to the same Arrhenius law as for the previously obtained data from the ac measurements ($\tau_{01} = 2.1 \times 10^{-10}$ s, $\Delta_{\tau 1} = 94.1$ K). Below 4.5 K, as shown in Figure 12, the relaxation deviates significantly from the previous linear behavior and adopts a second activated regime with $\tau_{02} = 6.8 \times 10^{-8}$ s and $\Delta_{\tau 2} = 67.7$ K. This type of crossover that has been observed experimentally only for a few compounds: $[Mn_2(saltmen)_2Ni(pao)_2(py)_2](ClO_4)_2$,[2e] $(NEt_4)[Mn_2(5\text{-MeOsalen})_2Fe(CN)_6]$[2f] (5-MeOsalen^{2-}: *N*,*N*′-ethylene-bis-(5-methoxysalicylideneiminate)), or [Dy(hfac)$_3$NIT(PhOPh)] (hfac: hexafluoroacetylacetonate, NIT(PhOPh): 2-(4′-phenoxy-benzyl)-4,4,5,5-tetramethylimidazoline-1-oxyl-3-oxide),[5d] is predicted when the correlation length (ξ) of the ideal infinite chain becomes larger than the real chain length (L)[33] that can be, for example, limited by the structural defects.

Discussion of the single-chain magnet behavior in compound 1: Despite the complexity of this system, we can still use general arguments to analyze the single-chain magnet behavior observed in compound **1**. The growth of the correlation length, ξ, is experimentally activated with $\Delta_\xi = 26.5$ K as expected for any anisotropic 1D model that favors an easy axis.[24–26] Taking $D_{Mn}/k_B = -2.4$ K and $J/k_B = -96.1$ K, compound **1** falls clearly in the regime where the domain walls possess a broad structure ($|D_{Mn}|S_{Mn}^2 \ll |J|S_{Mn}s_{rad}$). In this limit, the low-temperature thermodynamic properties may be influenced by several competing elementary excitations. In particular, the competing role of spin-waves and domain walls has been discussed by several authors.[25,26,34] From reference [26], Δ_ξ gives the energy to produce a domain wall along the chain even in the limit where the anisotropy is much smaller than the exchange energy. In general, Δ_ξ is a complex expression that is not clearly established, which depends in a complex manner on the type of spins, the exchange, and anisotropy energies. Nevertheless, the relaxation time of the magnetization is still activated with the corresponding energy gap (Δ_τ) expressed as $\Delta_{\tau 1} = \Delta_A + 2\Delta_\xi$ in the infinite chain regime, and as $\Delta_{\tau 2} = \Delta_A + \Delta_\xi$ at lower temperature when defects become relevant (where Δ_A is the energy barrier of the characteristic time describing the dynamics of a free-moving domain wall).[35] Indeed, experimentally, $\Delta_{\tau 1} - \Delta_{\tau 2} \approx 94.1 - 67.7 = 26.4$ K (Figure 12) is in excellent agreement with the Δ_ξ value (26.5 K) deduced from the $\ln(\chi T)$ versus $1/T$ plot (Figure 5). Moreover, the activation energy Δ_A can also be estimated to be about $\Delta_{\tau 2} - \Delta_\xi = 41.2$ K. This value is larger than the $|D_{Mn}|S_{Mn}^2 = 9.8$ K value, expected in the case of single-chain magnets possessing narrow domain walls.[2,35] This result can be qualitatively understood considering the presence of broad domain walls that involve collectively a series of neighboring spins. Therefore, the dynamics of these domains involve several anisotropic spins and thus it is not surprising to find that Δ_A is larger than $|D_{Mn}|S_{Mn}^2$. We show here that even without an analytical expression of Δ_ξ and Δ_A, a detailed comparison of the thermodynamic and dynamic properties allows an unambiguous analysis of a single-chain magnet.

Conclusion

We have described in this paper a new one-dimensional material, $[Mn(5\text{-TMAMsaltmen})(TCNQ)](ClO_4)_2$ (**1**), that is made of a well-isolated chain of a Mn^{III} salen derivative and the TCNQ radical. The synthesis, structure, and magnetic properties have been studied in detail. This compound falls in the family of materials reported by Miller and co-workers on the basis of its alternated Mn^{III}/rad chain structure. Indeed, the slow magnetization relaxation behavior of some of these systems based on Mn^{III} porphyrin complexes and the TCNE or TCNQ radicals has been observed before the discovery of the SCM systems. But in these materials, the presence of interstitial crystallization solvents, their disorder, or partial elimination, produce structural fluctuations in the

packing structure that was invoked to explain their slow relaxation in the frame of a spin-glass model. In fact, the study of these materials is even more complicated as their magnetic properties and slow relaxation are strongly solvent-dependent as shown by Miller and co-workers and also by our group for related materials. Hence in this research project, compound **1** seems to be the "ultimate" sample to probe the intrinsic magnetic properties of this type of chain due to its high stability in air and the absence of interstitial solvent molecules. Combined static (susceptibility, heat capacity) and dynamics (relaxation time of the magnetization) have been used to clearly establish the single-chain magnet behavior of compound **1**.

In the initial step in this work, the essential details necessary to explain SCM behavior were determined: 1) the uniaxial anisotropy introduced by the Mn^{III} ion in a 5-TMAM-saltmen ligand field: $D_{Mn}/k_B \approx -2.4$ K, and; 2) the strong intrachain antiferromagnetic coupling: $J/k_B \approx -96$ K. In the second step, we determined the activation energies of the correlation length (Δ_ξ) and of the relaxation time ($\Delta_{\tau 1}$ and $\Delta_{\tau 2}$) that have been coherently correlated to the presence of SCM behavior with broad domain walls. Following this unique result, our current research is devoted to the synthesis of Mn^{III}/TCNE materials using Mn^{III} salen analogues and porphyrin derivatives. Indeed based on the previously reported work by Miller and co-workers, the TCNE radical tends to yield relatively stronger couplings with Mn^{III} than $TCNQ^{\bullet -}$ (see Table 3 and Figure 4). Hence, keeping the same type of magnetic anisotropy introduced by the Mn^{III} building blocks, the enhancement of the intrachain interactions should help us to pursue our quest through the design of a single-chain magnet at high temperatures.

Experimental Section

General procedures and materials: All chemicals used during the synthesis were reagent grade. Solvents were distilled under N_2 atmosphere by using common drying agents before use. Li(TCNQ) was prepared according to the literature method in reference [36]. All procedures were carried out under N_2 atmosphere by using Schlenk techniques.

Synthesis of [Mn(5-TMAMsaltmen)(H_2O)$_2$](ClO_4)$_3$·H_2O: [Mn(5-TMAM-saltmen)(H_2O)$_2$](ClO_4)$_3$·H_2O as a precursor for compound **1** was synthesized by using the literature method.[37] $Mn(CH_3CO_2)_3$·$2H_2O$ (0.912 g, 3.40 mmol) was added to a solution containing 5-(trimethylammoniummethyl)salicylaldehyde chloride (1.362 g, 6.80 mmol) and NaOH (0.08 g, 2.00 mmol) in water (50 mL). The solution was then refluxed for 10 min before addition of a solution of 1,1,2,2-tetramethylethylenediamine dihydrochloride salt (0.643 g, 3.4 mmol) and NaOH (0.272 g, 6.4 mmol) in water (20 mL). The solution was refluxed for 20 min. Finally, $NaClO_4$ (2.081 g, 17 mmol) was added and then the solution was refluxed for an additional 30 min. The dark brown solution was filtered and left to stand for three days to yield a dark brown crystalline sample. After filtration, the crystals were washed with a small amount of H_2O and dried in vacuo. Yield 53.0% (based on Mn). Elemental analysis calcd (%) for [Mn(5-TMAM-saltmen)(H_2O)$_2$](ClO_4)$_3$·H_2O: C 38.48, H 5.54, N 6.41; found: C 38.64, H 5.34, N 6.44; IR (KBr): $\tilde{\nu}$ = 1616 (ν(C=N)); 1146, 1109, 1089 (ν(Cl−O)) cm^{-1}.

Synthesis of [Mn(5-TMAMsaltmen)(TCNQ)](ClO_4)$_2$ (1): A solution of Li(TCNQ) (42 mg, 0.2 mmol) in methanol (10 mL) was added to a solution of [Mn(5-TMAMsaltmen)(H_2O)](ClO_4)$_3$ (175 mg, 0.2 mmol) in acetonitrile (10 mL). The resulting dark-colored solution was immediately filtered and allowed to stand for about one week to form purplish-brown crystals of compound **1** (yield: 75 mg, 41%). Elemental analysis calcd (%) for compound **1**, $C_{40}H_{46}N_8O_{10}Cl_2Mn$: C 51.96, H 5.01, N 12.12; found: C 51.63, H 4.99, N 12.13; IR (KBr): $\tilde{\nu}$ = 2189, 2127 (ν(C≡N)); 1616, 1601 (ν(C=N)); 1121 (ν(Cl−O)) cm^{-1}.

Physical measurements: Infrared spectra were measured by using KBr disks with a Shimadzu FTIR-8600 spectrophotometer. Magnetic susceptibility measurements were obtained with a Quantum Design SQUID magnetometer MPMS-XL. The dc measurements were collected from 1.8 to 300 K and from −70 to 70 kOe. The ac measurements were performed at various frequencies from 1 to 1488 Hz with an ac field amplitude of 3 Oe and no dc field applied. The general measurements were performed on finely ground polycrystalline samples restrained with *n*-eicosane. Experimental data were also corrected for the sample holder and for the diamagnetic contribution calculated from Pascal constants.[38] Magnetization measurements on a single crystal were performed with an array of micro-SQUID instruments.[39] This magnetometer works in the temperature range 0.04 to ~7 K and in fields of up to 1.4 T with sweeping rates as high as 10 $T s^{-1}$, along with field stability better than microtesla. The time resolution was approximately 1 ms. The field could be applied in any direction of the micro-SQUID plane with precision much better than 0.1° by separately driving three orthogonal coils. In order to ensure good thermalization, a single crystal was fixed with Apiezon grease. Transverse-field magnetization measurements were performed with a home-built Hall probe magnetometer. The Hall probes (typically 10×10 μm^2) were made of two-dimensional GaAs/GaAsAl heterostructures and worked in the temperature range 1.5–100 K, and in magnetic fields of up to 16 T. Specific heat capacities were measured on a single crystal of compound **1** by a thermal relaxation technique in a ^{3}He cryostat (lowest temperature: 0.4 K), the detailed description of which was previously reported.[40] In each measurement, the blank heat capacity (including a small amount of Apiezon N grease (< 1 mg), which was used for adhesion) was measured prior to the sample mounting. The specific heat capacities were determined by subtracting the blank data fitted by polynomial functions from the measured total heat capacities.

Crystallography: A single crystal with dimensions of $0.20 \times 0.20 \times 0.10$ mm^3 of compound **1** was mounted on a glass rod. Data collections were made on a Rigaku CCD diffractometer (Saturn70) with graphite-monochromated $Mo_{K\alpha}$ radiation (λ = 0.71069 Å). The structures were solved by direct methods (SIR92)[41] and were expanded by using Fourier techniques (DIRDIF99).[42] The non-hydrogen atoms were refined anisotropically, while hydrogen atoms were introduced as fixed contributors. The crystal used was a non-merohedral twin and the obtained data were first treated by a special technique for twinned crystals. The twin component of the final material comprised 64.33% of the crystal. The final cycle of full-matrix least-squares refinement on F^2 was based on 5660 observed reflections and 278 variable parameters, and converged with unweighted and weighted agreement factors of $R_1 = \Sigma||F_o|-|F_c||/\Sigma|F_o|$ ($I > 2.00\sigma(I)$ and all reflections), and $wR_2 = [\Sigma w(F_o^2 - F_c^2)^2/\Sigma w(F_o^2)^2]^{1/2}$ (all reflections). A Sheldrick weighting scheme was used. Neutral atom scattering factors were taken from Cromer and Waber.[43] Anomalous dispersion effects were included in F_{calcd}; the values $\Delta f'$ and $\Delta f''$ were those of Creagh and McAuley.[44] The values for the mass attenuation coefficients were those of Creagh and Hubbel.[45] All calculations were performed by using the CrystalStructure crystallographic software package,[46] and final refinement for compound **1** was performed by using SHELXL-97.[47]

Crystal and experimental data for compound 1: $C_{40}H_{46}N_8O_{10}Cl_2Mn$, F_W = 924.69, monoclinic *C*2/*c* (no. 15), $T = (-150 \pm 1)$ °C, $\lambda(Mo_{K\alpha})$ = 0.71069 Å, a = 24.629(3), b = 15.348(2), c = 12.140(2) Å, β = 113.198(6)°, V = 4217.9(10) Å^3, Z = 4, ρ_{calcd} = 1.456 g cm^{-3}, F_{000} = 1924.00, $2\theta_{max}$ = 56.6°. Final R_1 = 0.063 ($I > 2.00\sigma(I)$), R = 0.068 (all reflections), wR_2 = 0.170, GOF = 1.170. The linear absorption coefficient, μ, for $Mo_{K\alpha}$ radiation is 5.07 cm^{-1}. An empirical absorption correction was applied that resulted in transmission factors ranging from 0.2583 to 1.0000. The data were corrected for Lorentz and polarization effects. Max positive and negative peaks in the ΔF map were found to be ρ_{max} and ρ_{min} = 0.43 and −0.47 e Å^{-3}, respectively.

CCDC-294990 contains the supplementary crystallographic data (excluding structure factors) for the structure of compound **1** for this paper. These data can be obtained free of charge from the Cambridge Crystallographic Data Centre via www.ccdc.cam.ac.uk/data_request/cif.

Acknowledgements

We acknowledge Dr. A. Vindigni (ETH-Zürich, Switzerland) for helpful discussions. This work was financially supported by the PRESTO and CREST projects, Japan Science and Technology Agency (JST), and a Grant-in-Aid for Scientific Research on Priority Areas (No 17036054 "Chemistry of Coordination Space") from the Ministry of Education, Science, Sports, and Culture, Japan. R.C. and C.C. would like to thank the CNRS, the University of Bordeaux 1, the Conseil Regional d'Aquitaine, and MAGMANet (NMP3-CT-2005-515767) for financial support.

[1] a) A. Caneschi, D. Gatteschi, N. Lalioti, C. Sangregorio, R. Sessoli, G. Venturi, A. Vindigni, A. Rettori, M. G. Pini, M. A. Novak, *Angew. Chem.* **2001**, *113*, 1810; *Angew. Chem. Int. Ed.* **2001**, *40*, 1760; b) A. Caneschi, D. Gatteschi, N. Lalioti, C. Sangregorio, R. Sessoli, G. Venturi, A. Vindigni, A. Rettori, M. G. Pini, M. A. Novak, *Europhys. Lett.* **2002**, *58*, 771; c) L. Bogani, A. Caneschi, M. Fedi, D. Gatteschi, M. Massi, M. A. Novak, M. G. Pini, A. Rettori, R. Sessoli, A. Vindigni, *Phys. Rev. Lett.* **2004**, *92*, 207204; d) L. Bogani, R. Sessoli, M. G. Pini, A. Rettori, M. A. Novak, P. Rosa, M. Massi, M. Fedi, L. Giuntini, A. Caneschi, D. Gatteschi, *Phys. Rev. B* **2005**, *72*, 064406; e) A. Vindigni, A. Rettori, L. Bogani, A. Caneschi, D. Gatteschi, R. Sessoli, M. A. Novak, *Appl. Phys. Lett.* **2005**, *87*, 073102; f) A. Vindigni, A. Rettori, M. G. Pini, C. Carbone, P. Gambardella, *Appl. Phys. A* **2005**, *87*, 073102.

[2] a) R. Clérac, H. Miyasaka, M. Yamashita, C. Coulon, *J. Am. Chem. Soc.* **2002**, *124*, 12837; b) H. Miyasaka, R. Clérac, K. Mizushima, K. Sugiura, M. Yamashita, W. Wernsdorfer, C. Coulon, *Inorg. Chem.* **2003**, *42*, 8203; c) C. Coulon, R. Clérac, L. Lecren, W. Wernsdorfer, H. Miyasaka, *Phys. Rev. B* **2004**, *69*, 132408; d) H. Miyasaka, R. Clérac, *Bull. Chem. Soc. Jpn.* **2005**, *78*, 1725; e) W. Wernsdorfer, R. Clérac, C. Coulon, L. Lecren, H. Miyasaka, *Phys. Rev. Lett.* **2005**, *95*, 237203; f) M. Ferbinteanu, H. Miyasaka, W. Wernsdorfer, K. Nakata, K. Sugiura, M. Yamashita, C. Coulon, R. Clérac, *J. Am. Chem. Soc.* **2005**, *127*, 3090; g) H. Miyasaka, T. Nezu, K. Sugimoto, K.-i. Sugiura, M. Yamashita, R. Clérac, *Chem. Eur. J.* **2005**, *11*, 1592.

[3] R. Lescouëzec, J. Vaissermann, C. Ruiz-Pérez, F. Lloret, R. Carrasco, M. Julve, M. Verdaguer, Y. Dromzee, D. Gatteschi, W. Wernsdorfer, *Angew. Chem.* **2003**, *115*, 1521; *Angew. Chem. Int. Ed.* **2003**, *42*, 1483.

[4] T. Liu, D. Fu, S. Gao, Y. Zhang, H. Sun, G. Su. Y. Liu, *J. Am. Chem. Soc.* **2003**, *125*, 13976.

[5] a) F. Chang, S. Gao, H.-L. Sun, Y.-L. Hou, G. Su, *Proceedings of the ICSM Conference* (Shanghai, China) **2002** p. 182; b) R. Lescouëzec, J. Vaissermann, C. Ruiz-Pérez, F. Lloret, R. Carrasco, M. Julve, M. Verdaguer, Y. Dromzee, D. Gatteschi, W. Wernsdorfer, *Angew. Chem.* **2003**, *115*, 1521; *Angew. Chem. Int. Ed.* **2003**, *42*, 1483; c) L. M. Toma, R. Lescouëzec, F. Lloret, M. Julve, J. Vaissermann, M. Verdaguer, *Chem. Commun.* **2003**, 1850; d) L. Bogani, C. Sangregorio, R. Sessoli, D. Gatteschi, *Angew. Chem.* **2005**, *117*, 5967; *Angew. Chem. Int. Ed.* **2005**, *44*, 5817.

[6] a) E. Pardo, R. Ruiz-Garcia, F. Lloret, J. Faus, M. Julve, Y. Journaux, F. Delgado, C. Ruiz-Perez, *Adv. Mater.* **2004**, *16*, 1597; b) Z.-M. Sun, A. V. Prosvirin, H.-H. Zhao, J.-G. Mao, K. R. Dunbar, *J. Appl. Phys.* **2005**, *97*, 10B305; c) T. Kajiwara, M. Nakano, Y. Kaneko, S. Takaishi, T. Ito, M. Yamashita, A. Igashira-Kamiyama, H. Nojiri, Y. Ono, N. Kojima, *J. Am. Chem. Soc.* **2005**, *127*, 10150; d) N. Shaikh, A. Panja, S. Goswami, P. Banerjee, P. Vojtysek, Y.-Z. Zhang, G. Su, S. Gao, *Inorg. Chem.* **2004**, *43*, 849; e) S. Wang, J.-L. Zuo, S. Gao, Y. Song, H.-C. Zhou, Y.-Z. Zhang, X.-Z. You, *J. Am. Chem. Soc.* **2004**, *126*, 8900; f) J. P. Costes, J. M. Clemente-Juan, F. Dahan, J. Milon, *Inorg. Chem.* **2004**, *43*, 8200.

[7] N. E. Chakov, W. Wernsdorfer, K. A. Abboud, G. Christou, *Inorg. Chem.* **2004**, *43*, 5919.

[8] R. J. Glauber, *J. Math. Phys.* **1963**, *4*, 294.

[9] a) G. Christou, D. Gatteschi, D. N. Hendrickson, R. Sessoli, *MRS Bull.* **2000**, 66; b) D. Gatteschi, R. Sessoli, *Angew. Chem.* **2003**, *115*, 278; *Angew. Chem. Int. Ed.* **2003**, *42*, 268.

[10] Considering the following definition of the anisotropic terms: $H_{aniso} = DS_{T_z}{}^2 + E(S_{T_z} - S_{T_z})$.

[11] a) D. A. Summerville, T. W. Cape, E. D. Johnson, F. Basolo, *Inorg. Chem.* **1978**, *17*, 3297; b) J. S. Miller, J. C. Calabrese, R. S. McLean, A. J. Epstein, *Adv. Mater.* **1992**, *4*, 498; c) P. Zhou, B. G. Morin, A. J. Epstein, R. S. McLean, J. S. Miller, *J. Appl. Phys.* **1993**, *73*, 6569; d) J. S. Miller, C. Vazquez, J. C. Calabrese, S. McLean, A. J. Epstein, *Adv. Mater.* **1994**, *6*, 217; e) J. S. Miller, C. Vazquez, N. L. Jones, R. S. McLean, A. J. Epstein, *J. Mater. Chem.* **1995**, *5*, 707; f) W. B. Brinckerhoff, B. G. Morin, E. J. Brandon, J. S. Miller, A. J. Epstein, *J. Appl. Phys.* **1996**, *79*, 6147; g) A. Bohm, C. Vazquez, R. S. Mclean, J. C. Calabrese, S. E. Kalm, J. L. Manson, A. J. Epstein, J. S. Miller, *Inorg. Chem.* **1996**, *35*, 3083; h) J. S. Miller. A. J. Epstein, *Chem. Commun.* **1998**, 1319; i) E. J. Brandon, C. Kollmar, J. S. Miller, *J. Am. Chem. Soc.* **1998**, *120*, 1822; j) E. J. Brandon, D. K. Rittenberg, A. M. Arif, J. S. Miller, *Inorg. Chem.* **1998**, *37*, 3376; k) E. J. Brandon, A. M. Arif, B. M. Burkhart, J. S. Miller, *Inorg. Chem.* **1998**, *37*, 2792; l) D. K. Rittenberg, J. S. Miller, *Inorg. Chem.* **1999**, *38*, 4838; m) D. K. Rittenberg, K. Sugiura, Y. Sakata, I. A. Guzei, A. L. Rheingold, J. S. Miller, *Chem. Eur. J.* **1999**, *5*, 1874; n) D. K. Rittenberg, L. Baars-Hibbe, A. Böhm, J. S. Miller, *J. Mater. Chem.* **2000**, *10*, 241; o) J. S. Miller, *Inorg. Chem.* **2000**, *39*, 4393.

[12] a) K. Sugiura, S. Mikami, M. T. Johnson, J. S. Miller, K. Iwasaki, K. Umishita, S. Hino, Y. Sakata, *J. Mater. Chem.* **2000**, *10*, 959; b) M. T. Johnson, A. M. Arif, J. S. Miller, *Eur. J. Inorg. Chem.* **2000**, *6*, 1781.

[13] a) C. M. Wynn, M. A. Girtu, W. B. Brinckhoff, K.-i. Sugiura, J. S. Miller, A. J. Epstein, *Chem. Mater.* **1997**, *9*, 2156; b) C. M. Wynn, M. A. Girtu, J. S. Miller, A. J. Epstein, *Phys. Rev. B* **1997**, *56*, 315; c) C. M. Wynn, M. A. Girtu, J. S. Miller, A. J. Epstein, *Phys. Rev. B* **1997**, *56*, 14050.

[14] E. J. Brandon, R. D. Rogers, B. M. Burkhart, J. S. Miller, *Chem. Eur. J.* **1998**, *4*, 1938.

[15] K. Sugiura, S. Mikami, M. T. James, J. W. Raebiger, J. S. Miller, K. Iwasaki, Y. Okada, S. Hino, Y. Sakata, *J. Mater. Chem.* **2001**, *11*, 2152.

[16] a) S. J. Etzkorn, W. Hibbs, J. S. Miller, A. J. Epstein, *Phys. Rev. Lett.* **2002**, *89*, 207201; b) S. J. Etzkorn, W. Hibbs, J. S. Miller, A. J. Epstein, *Phys. Rev. B* **2004**, 70, 134419

[17] W. Hibbs, D. K. Rittenberg, K. Sugiura, B. M. Burkhart, B. G. Morin, A. M. Arif, L. Liable-Sands, A. L. Rheingold, M. Sundaralingam, A. J. Epstein, J. S. Miller, *Inorg. Chem.* **2001**, *40*, 1915.

[18] M. S. Khatkale, J. P. Devlin, *J. Chem. Phys.* **1979**, *70*, 1851.

[19] T. J. Kistenmacher, T. J. Emge, A. N. Bloch, D. O. Cowan, *Acta Crystallogr. Sect. B* **1982**, *38*, 1193.

[20] R. E. Long, R. A. Sparks, K. N. Trueblood, *Acta Crystallogr.* **1965**, *21*, 932.

[21] A. Hoekstra, T. Spoelder, A. Vos, *Acta Crystallogr. Sect. B* **1972**, *28*, 14.

[22] J. Seiden, *J. Physique Lett.* **1983**, *44*, L947.

[23] E. J. Brandon, C. Kollmar, J. S. Miller, *J. Am. Chem. Soc.* **1998**, *120*, 1822.

[24] J. M. Loveluck, S. W. Lovesey, S. Aubry, *J. Phys. C* **1975**, *8*, 3841.

[25] K. Nakamura, T. Sasada, *J. Phys. C* **1978**, *11*, 331.

[26] K. Nakamura, T. Sasada, *Solid State Commun.* **1977**, *21*, 891.

[27] B. Barbara, *J. Physique* **1973**, *34*, 1034; B. Barbara, *J. Magn. Magn. Mater.* **1994**, *129*, 79.

[28] The minimization of E_{eff} is obtained by simple derivation: $dE_{eff}/d\theta = 0$ and we called θ_{min} the resulting angle.

[29] a) H. Miyasaka, R. Clérac, T. Ishii, H.-C. Chang, S. Kitagawa, M. Yamashita, *J. Chem. Soc. Dalton Trans.* **2002**, 1528; b) H. Miyasaka, R. Clérac, W. Wernsdorfer, L. Lecren, C. Bonhomme, K.-i. Sugiura,

M. Yamashita, *Angew. Chem.* **2004**, *116*, 2861; *Angew. Chem. Int. Ed.* **2004**, *43*, 2801.
[30] a) A. M. Gomes, M. A. Novak, R. Sessoli, A. Caneschi, D. Gatteschi, *Phys. Rev. B* **1998**, *57*, 5021; b) F. Fominaya, J. Villain, T. Fournier, P. Gandit, J. Chaussy, A. Fort, A. Caneschi, *Phys. Rev. B* **1999**, *59*, 519; c) Y. Miyazaki, A. Bhattacharjee, M. Nakano, K. Saito, S. M. J. Aubin, H. J. Eppley, G. Christou, D. N. Hendrickson, M. Sorai, *Inorg. Chem.* **2001**, *40*, 6632; d) A. Bhattacharjee, Y. Miyazaki, M. Nakano, J. Yoo, G. Christou, D. N. Hendrickson, M. Sorai, *Polyhedron* **2001**, *20*, 1607; e) A. Yamaguchi, N. Kusumi, H. Ishimoto, H. Mitamura, T. Goto, N. Mori, M. Nakano, K. Awaga, J. Yoo, D. N. Hendrickson, G. Christou, *J. Phys. Soc. Jpn.* **2002**, *71*, 414.
[31] H. Miyasaka and co-workers, unpublished results.
[32] a) K. S. Cole, R. H. Cole, *J. Chem. Phys.* **1941**, *9*, 341; b) C. J. F. Boettcher, *Theory of Electric Polarisation*, Elsevier, Amsterdam, **1952**; c) S. M. Aubin, Z. Sun, L. Pardi, J. Krzysteck, K. Folting, L.-J. Brunel, A. L. Rheingold, G. Christou, D. N. Hendrickson, *Inorg. Chem.* **1999**, *38*, 5329–5340.
[33] a) J. K. Leal da Silva, A. G. Moreira, M. S. Soares, F. C. S. Barreto, *Phys. Rev. E* **1995**, *52*, 4527; b) J. H. Luscombe, M. Luban, J. P. Reynolds, *Phys. Rev. E* **1996**, *53*, 5852.
[34] a) T. Sakai, M. Matsumoto, K. Asakura, M. Sato, *Prog. Theor. Phys. Suppl.* **2005**, *159*, 308; b) Y. Oshima, H. Nojiri, K. Asakura, T. Sakai, M. Yamashita, H. Miyasaka, *Phys. Rev. B* **2006**, in press.
[35] C. Coulon, H. Miyasaka, R. Clérac, *Structure and Bonding* **2006**, *122*, 163–206.
[36] L. R. Melby, R. J. Harder, W. R. Hertler, W. Mahler, R. E. Benson, W. E. Mochel, *J. Am. Chem. Soc.* **1962**, *84*, 3374.
[37] F. Sakamoto, T. Sumiya, M. Fujita, T. Tada, X. S. Tan, E. Suzuki, I. Okura, Y. Fujii, *Chem. Lett.* **1998** 1127.
[38] E. A. Boudreaux, L. N. Mulay, *Theory and Applications of Molecular Paramagnetism*, Wiley, New York, **1976**.
[39] W. Wernsdorfer, *Adv. Chem. Phys.* **2001**, *118*, 99.
[40] M. Ishikawa, Y. Nakazawa, T. Takabatake, A. Kishi, R. Kato, A. Maesono, *Solid State Commun.* **1988**, *66*, 201.
[41] SIR97: A. Altomare, G. Cascarano, C. Giacovazzo, A. Guagliardi, M. Burla, G. Polidori, M. Camalli, *J. Appl. Crystallogr.* **1994**, *27*, 435.
[42] DIRDIF99: P. T. Beurskens, G. Admiraal, G. Beurskens, W. P. Bosman, R. de Gelder, R. Israel, J. M. M. Smits. The DIRDIF-99 Program System, Technical Report of the Crystallography Laboratory, University of Nijmengen, The Netherlands, **1999**.
[43] D. T. Cromer, J. T. Waber, *International Tables for Crystallography, Vol. IV*, The Kynoch Press, Birmingham, England, Table 2.2A, **1974**.
[44] D. C. Creagh, W. J. McAuley, *International Tables for Crystallography, Vol. C* (Ed.: A. J. C. Wilson), Kluwer Academic Publishers, Boston, Table 4.2.6.8, pp. 219–222, **1992**.
[45] D. C. Creagh, J. H. Hubbell, *International Tables for Crystallography Vol. C* (Ed.: A. J. C. Wilson), Kluwer Academic Publishers, Boston, Table 4.2.4.3, pp. 200–206, **1992**.
[46] CrystalStructure 3.15: Crystal Structure Analysis Package, Rigaku and Rigaku/MSC (2000–2002). 9009 New Trails Dr., The Woodlands, TX 77381, USA.
[47] G. M. Sheldrick, SHELX97, **1997**.

Received: March 2, 2006
Published online: August 7, 2006

